Water Research 301 (2026) 126056

Contents lists available at ScienceDirect

Water Research

journal homepage: www.elsevier.com/locate/watres

Microplastics deplete soil available nutrients: a global meta-analysis with machine learning reveals critical thresholds and interactive controls

Yangzhou Xiang [a], Josep Peñuelas [b,c], Matthias C. Rillig [d], Xuqiang Luo [a], Luca Nizzetto [e], Jarkko Akkanen [f], Ying Liu [g], Yang Luo [a], Bin Yao [h,*], Yuan Li [i,*]

[a] School of Geography and Resources, Guizhou Education University, Guiyang 550018, China
[b] CSIC Global Ecology Unit, CREAF-CSIC-UAB, 08193 Bellaterra, Catalonia, Spain
[c] CREAF - Ecological and Forestry Applications Research Centre, 08193 Cerdanyola del Vallès, Catalonia, Spain
[d] Institut für Biologie, Berlin-Brandenburg Institute of Advanced Biodiversity Research (BBIB), Freie Universität Berlin, Berlin D-14195, Germany
[e] Norwegian Institute for Water Research, Økernveien 94, 0579 Oslo, Norway
[f] Department of Environmental and Biological Sciences, University of Eastern Finland, Joensuu, Finland
[g] School of Biological Sciences, Guizhou Education University, Guiyang 550018, China
[h] State Key Laboratory of Tree Genetics and Breeding, Institute of Ecology Conservation and Restoration, Chinese Academy of Forestry, Beijing 100091, China
[i] Grasslands and Sustainable Farming, Production Systems Unit, Natural Resources Institute Finland, Halolantie 31 A, 71750, Maaninka, Finland

HIGHLIGHTS

- MPs deplete soil nutrients: P –9.4% > K –7.0% > N –5.3% (206 studies, n = 2853).
- Effects are context-specific: pot/incubation show depletion, field studies do not.
- Machine learning identifies pH, MP concentration as hierarchical nutrient controls.
- Soil pH flips MP effects: N –31.7% in acidic *vs* +20.3% in alkaline soils.
- Biodegradable MPs match or exceed conventional ones in depleting soil nutrients.

GRAPHICAL ABSTRACT

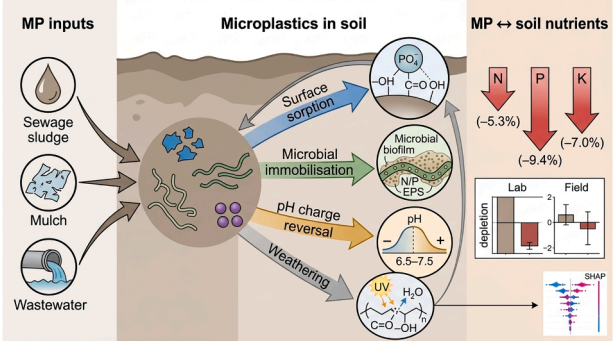

ARTICLE INFO

Keywords:
Soil–water interface
Nutrient bioavailability
Meta-analysis
Machine learning
Sorption dynamics

ABSTRACT

Microplastics (MPs) contamination threatens soil nutrient bioavailability, yet quantitative understanding of effect magnitudes and controlling factors remains fragmented across diverse environmental contexts. Here, we synthesized 206 studies (2853 observations) spanning 12 countries and diverse agricultural systems (soil pH 4.5–8.5; organic matter 5–80 g kg^{-1}) to quantify MPs impacts on soil available nitrogen (AN), phosphorus (AP), and potassium (AK). We integrated random-effects meta-analysis using log response ratios (ln*RR*) with eXtreme Gradient Boosting (XGBoost) machine learning interpreted through SHapley Additive exPlanations (SHAP) to identify non-linear relationships and interactive controls. The dataset comprised predominantly controlled experiments (pot: 49%; incubation: 50%; field: 1%), with geographical concentration in East Asia (92%). Across all experimental setups, MPs significantly depleted AN by 5.3%, AP by 9.4%, and AK by 7.0% relative to controls.

* Corresponding authors.
E-mail addresses: acmn21@caf.ac.cn (B. Yao), yuan.li@luke.fi (Y. Li).

https://doi.org/10.1016/j.watres.2026.126056
Received 9 January 2026; Received in revised form 25 April 2026; Accepted 1 May 2026
Available online 2 May 2026

However, effects were context-dependent: pot/incubation studies showed significant depletion, while field studies reported no significant changes. XGBoost models (R^2 = 0.44–0.62) indicated hierarchical control structures, with soil pH dominating AN responses (relative importance: 18.4%) and MPs concentration governing AP (15.2%) and AK (14.8%). SHAP analysis identified critical thresholds: particle size effects plateaued above 100 μm, concentration impacts saturated beyond 10 g kg^{-1}, and pH-dependent reversals shifted from depletion in acidic soils to enrichment under alkaline conditions. Biodegradable plastics (*e.g.*, PLA, PBAT) caused equal or greater short-term nutrient immobilization than conventional polymers, though mechanisms likely differ: biodegradable MPs may stimulate microbial biomass growth that temporarily sequesters nutrients, whereas conventional plastics primarily act through surface sorption. Partial dependence analysis indicated synergistic interactions: small particles (<50 μm) combined with high concentrations (>30 g kg^{-1}) induced depletion 1.5–2.3-fold beyond additive expectations. These findings establish quantitative thresholds for risk assessment and demonstrate that MPs-induced nutrient limitation, observed primarily in controlled settings, could affect crop yields, necessitating interventions to prevent irreversible soil fertility degradation, though field-scale validation remains essential.

1. Introduction

Microplastics (MPs) contamination has emerged as a threat to terrestrial ecosystems, with agricultural soils receiving an estimated 63,000–430,000 tons annually through plastic mulch fragmentation, sewage sludge application, irrigation, and atmospheric deposition (Nizzetto et al., 2016; Zhang et al., 2020). These persistent pollutants, defined as plastic particles < 5 mm in diameter, accumulate in agricultural systems at concentrations reaching 43,000 particles kg^{-1} soil (Fuller and Gautam, 2016), yet their impacts on soil nutrient bioavailability, the foundation of global food security, remain poorly quantified across diverse environmental contexts.

Soil available nutrients, particularly nitrogen (N), phosphorus (P), and potassium (K), constitute the primary limiting factors for crop production, with their bioavailability governing agricultural yields that sustain 8 billion people (Mueller et al., 2012). These nutrients exist in dynamic equilibrium mediated by complex interactions among soil minerals, organic matter, and microbial communities (Hinsinger et al., 2011). MPs potentially disrupt these equilibria through multiple mechanisms: direct sorption onto polymer surfaces, altered soil physical structure affecting water and nutrient transport, release of plastic additives toxic to soil biota, and modification of microbial community composition and function (de Souza Machado et al., 2018; Rillig et al., 2019; Wang et al., 2023, 2022). However, the relative importance of these mechanisms and their dependence on MPs characteristics and environmental conditions remain unresolved.

Previous studies have yielded contradictory results, with studies reporting enhancement, suppression, or neutral effects on nutrient availability (Chen et al., 2022; de Souza Machado et al., 2019). This variability likely reflects heterogeneity in experimental conditions, including differences in polymer types (ranging from biodegradable polylactic acid to persistent polyvinyl chloride), particle characteristics (sizes ranging from 50 μm to 5 mm), exposure conditions (laboratory incubations to multi-season field trials), and soil properties (pH 4.5–8.5, organic matter 5–80 g kg^{-1}) (Fan et al., 2022; Yu et al., 2022). While recent meta-analyses have addressed specific aspects such as N cycling or carbon dynamics (Lan et al., 2025; Xiang et al., 2024), none have comprehensively quantified MPs impacts across the complete N-P-K continuum while accounting for interactive environmental controls.

Environmental context fundamentally affects microplastic-soil interactions through multiple pathways. Temperature affects polymer degradation rates and microbial activity, with climate warming potentially accelerating MPs breakdown and additive release (Afzal et al., 2025; Seeley et al., 2020). Soil pH controls surface charge of both MPs and nutrients, determining electrostatic interactions that govern sorption-desorption dynamics (Joo et al., 2021). Clay content and organic matter influence aggregation processes that physically sequester MPs and associated nutrients (Lehmann et al., 2021). Furthermore, biological factors including plant roots create hotspots of enhanced microplastic-nutrient interactions through bioturbation and rhizosphere processes (Boots et al., 2019; Iqbal et al., 2024a). These multifaceted interactions warrant analytical approaches capable of capturing non-linear relationships and threshold effects invisible to traditional linear statistical methods.

Recent advances in machine learning offer opportunities to assess complex environmental interactions, with algorithms such as eXtreme Gradient Boosting (XGBoost) suggesting superior performance in capturing non-linear relationships and interaction effects in ecological datasets (Chen and Guestrin, 2016). When coupled with interpretable machine learning methods like SHAP (Shapley Additive Explanations), these approaches enable identification of hierarchical control structures and critical thresholds governing system response (Chen and Guestrin, 2016; Lundberg and Lee, 2017). Integration of machine learning with traditional meta-analysis could reveal previously hidden patterns essential for risk assessment and management strategy development.

This study integrated a global meta-analysis with machine learning to quantify MPs impacts on soil nutrient availability. We aimed to: (1) quantify overall effects of MPs exposure on available N, P, and K across diverse agricultural systems; (2) identify how experimental conditions, MPs characteristics, and edaphic properties affect nutrient responses; (3) employ machine learning to reveal non-linear relationships, threshold effects, and synergistic interactions governing MPs impacts; and (4) establish quantitative risk thresholds for evidence-based management interventions. We hypothesized that MPs would generally reduce available nutrients, with effects amplified by smaller particle sizes (<50 μm), higher concentrations (>10 g kg^{-1}), and increased temperatures (>27 °C) due to enhanced surface sorption and microbial disruption, while soil pH would moderate effect direction through regulation of polymer surface charge and nutrient speciation in soil solution.

2. Materials and methods

2.1. Literature search and screening, and data collection

A systematic literature search was conducted following PRISMA guidelines (Page et al., 2021) using Web of Science (http://www.webofknowledge.com), Google Scholar (http://scholar.google.com), and China National Knowledge Infrastructure (https://www.cnki.net) databases through May 28, 2025. The search strategy combined terms related to microplastics, soil, and available nutrients using Boolean operators: (microplastic* OR “plastic microparticles”) AND (soil) AND (“available nitrogen” OR “available N” OR “available phosphorus” OR “available P” OR “available potassium” OR “available K”). No language restrictions were applied during initial searches, with non-English articles translated for screening and data extraction.

Studies were included if they met the following criteria: (1) reported at least one target response variable (available nitrogen [AN], available phosphorus [AP], or available potassium [AK]); (2) included both control (no microplastic exposure) and treatment groups; (3) provided

means with standard deviation (SD) or standard error (SE); (4) included sample size (n ≥ 3 replicates) for each treatment; (5) represented independent datasets (when multiple publications reported identical experiments, the most comprehensive was retained). Studies were excluded if they: (1) lacked quantifiable data; (2) involved non-soil matrices (*e.g.*, aquatic sediments, hydroponic systems). This process yielded 206 studies containing 664 observations for AN, 1631 for AP, and 558 for AK (Fig. S1, Notes S1). The dataset showed experimental context heterogeneity: pot experiments contributed 49% of observations (AN: 326; AP: 839; AK: 353), incubations 50% (AN: 332; AP: 771; AK: 199), and field studies 1% (AN: 6; AP: 21; AK: 6). This composition enables mechanistic inference while requiring cautious field-scale extrapolation.

2.2. Data extraction and categorization

For each observation, we recorded: means, dispersion measures (SD/SE), and sample sizes for treatment and control groups. When only SE was reported, conversion to SD was performed using $SD = SE \times \sqrt{n}$. Data presented graphically were digitized using WebPlotDigitizer v4.6 with validation through duplicate extraction.

From each included study, we extracted response variables (AN, AP, AK) and potential affecting factors classified into three categories:

Experimental factors: experimental setup (ES; field, pot, incubation) (Liao et al., 2022); soil stress status (SS: pristine, contaminated with organics or heavy metals); exposure temperature (ET: 25 °C, 25–27 °C, 27 °C) (Xiang et al., 2023); exposure duration (ED: 30, 30–60, 60 days) (Zhao et al., 2024); plant involvement (present, absent) (Xiang et al., 2024); nitrogen fertilization (NYN: yes, no).

Microplastic characteristics: polymer composition (PC: poly (butylene adipate-co-terephthalate) [PBAT], polyethylene [PE], polystyrene [PS], polyvinyl chloride [PVC], polylactic acid [PLA], polypropylene [PP], polyethylene terephthalate [PET], other) (Xiang et al., 2023); MPs type (MPT: virgin, aged); MPs biodegradability (MPB: conventional, biodegradable) (Su et al., 2024); MPs size (MPS: 50 μm [small], 50–150 μm [medium], > 150 μm [large]) (Xiang et al., 2025); MPs concentration (MPC: < 10 [low], 10–30 [medium], > 30 g kg^{-1} [high]) (Xiang et al., 2025).

Edaphic properties: water holding capacity (WHC: < 50%, 50–70%, > 70%); soil clay content (SCC: < 10%, 10–20%, > 20%) (Xiang et al., 2025); initial soil pH (ISpH: < 5.5, 5.5–6.5, 6.5–7.5, 7.5–8.5, ≥ 8.5) (Wei et al., 2017); initial soil organic matter (ISOM: < 10, 10–20, 20–30, 30–40, ≥ 40 g kg^{-1}). Categories were established based on standard soil classification systems and distribution of values within the dataset to ensure adequate subgroup sizes.

2.3. Effect size calculation and meta-analysis

To assess the effect of MPs on soil available nutrients, we employed the natural logarithm of the response ratio (ln*RR*). This ratio represents the value of the variable in MPs-treated groups divided by its value in control groups as follows (Hedges et al., 1999):

$$lnRR = ln(\overline{X}_t / \overline{X}_c) = ln(\overline{X}_t) - ln(\overline{X}_c) \quad (1)$$

where $\overline{X}_t, \overline{X}_c$ show the corresponding mean soil available nutrient values for the MPs- exposure and control groups.

When multiple treatments utilize the identical control group in an experiment, the independence assumption is invalid (Knapp and van der Heijden, 2018). Thus, to handle non-dependence among sampling variances of within-study effect sizes (*e.g.*, resulting from shared control groups) in restricted maximum likelihood (REML) estimates (Freitas et al., 2025), a variance-covariance (VCV) matrix was implemented to specify covariances between sampling errors using the following equation (Knapp and van der Heijden, 2018):

$$VCV = \begin{bmatrix} \frac{(S_C)^2}{N_C \overline{X}_C^2} + \frac{(S_T^A)^2}{N_T^A (\overline{X}_T^A)^2} & \frac{(S_C)^2}{N_C (\overline{X}_C)^2} \\ \frac{(S_C)^2}{N_C (\overline{X}_C)^2} & \frac{(S_C)^2}{N_C \overline{X}_C^2} + \frac{(S_T^B)^2}{N_T^B (\overline{X}_T^B)^2} \end{bmatrix} \quad (2)$$

where $S_C, S_T^A, and S_T^B$ represent the standard deviations; $N_C, N_T^A, and N_T^B$ represent the sample sizes; $\overline{X}_C, \overline{X}_T^A, and \overline{X}_T^B$ represent the mean values of the measured variable for the control group, MPs-treated group A, and MPs-treated group B, respectively. The VCV matrix was generated using the 'covariance_commonControl ()' function in the "*metagear*" package version 0.7 (Lajeunesse, 2016).

Statistical significance of the effect of MPs exposure on the response variables (soil AN, AP, and AK) is indicated when the 95% confidence interval (CI) does not include zero. On the contrary, overlap between the CI and zero suggests a non-significant effect. Furthermore, to evaluate whether the effects of MPs exposure on soil available nutrients (AN, AP, and AK) varied across different experimental conditions, MP characteristics, and edaphic properties, we analyzed between-group heterogeneity (Q_M) using chi-squared tests. The presence of significant between-group heterogeneity (Q_M, $p < 0.05$) would provide statistical evidence for divergent effect sizes among these categorical moderators (Hedges et al., 1999). To facilitate interpretation, the weighted ln*RR* (RR_{++}) and its 95% CI was expressed as a percentage change using the following equation: Effect sizes (%) = $[\exp(RR_{++})-1)] \times 100$.

2.4. Publication bias and sensitivity analysis

To further ensure the stability and credibility of our results, we conducted a sensitivity analysis using a leave-one-out method in the "*metagear*" package version 4.6.0 (Viechtbauer, 2010), systematically evaluating the impact of each study on the overall effect size (Table S1, Fig. S3–4). We assessed publication bias through funnel plots and statistically evaluated it using Egger's regression test (Sterne and Egger, 2001). Additionally, we employed the trim-and-fill method (Duval and Tweedie, 2000) to estimate potential missing studies and adjust the effect sizes, thereby reinforcing the conclusions of our meta-analysis. All statistical analyses were conducted in R (version 4.3.3) (R Core Team, 2024).

2.5. Machine learning analysis

2.5.1. Data preprocessing

For machine learning analysis, continuous moderators (ED, particle size, concentration, temperature, pH, organic matter, WHC, clay content) were retained as numeric variables, while categorical variables were one-hot encoded. Missing values (< 5% of dataset) were imputed using median (continuous) or mode (categorical) values. The dataset was split 80:20 for training and testing, stratified by study identity to prevent data leakage.

2.5.2. Model development and selection

Five algorithms were compared: boosted regression trees (BRT; "*gbm*" v2.1.9), extreme gradient boosting (XGBoost; "*xgboost*" v1.7.3) (Chen and Guestrin, 2016), random forest (RF; "*randomForest*" v4.7–1) (Liaw and Wiener, 2002), multilayer perceptron (MLP; "*nnet*" v7.3–19) (Bergmeir and Benítez, 2012), and support vector machine (SVM; "*e1071*" v1.7–14) (Suthaharan, 2016). Hyperparameters were optimized via grid search with 10-fold cross-validation. For XGBoost, the search space included: learning rate (0.01–0.3), maximum depth (3–10), and number of rounds (50–500). Model performance was evaluated using coefficient of determination (R^2) and root mean square error (RMSE). Permutation testing (1000 iterations) confirmed feature importance scores exceeded null distributions ($p < 0.001$ for top-5

features). Leave-study-out cross-validation maintained comparable performance (mean R^2 reduction: 0.04±0.02), indicating predictions do not rely on study-specific artifacts. Hyperparameter tuning outcomes for all five algorithms are reported in Table S2.

2.5.3. Model interpretation

Feature importance was quantified using XGBoost's gain metric, representing the improvement in accuracy brought by each feature. SHAP ("*SHAPforxgboost*" v0.1.0) (Liu and Just, 2019) values were calculated to determine feature contributions and directionality for individual predictions(Lundberg and Lee, 2017). Partial dependence plots ("*pdp*" v0.8.1) (Greenwell, 2017) visualized marginal effects of individual predictors and two-way interactions, with 95% confidence intervals generated through bootstrapping (n = 1000).

2.6. Statistical analyses

Structural equation modeling (SEM) was employed to disentangle direct and indirect pathways through which experimental conditions, MPs characteristics, and edaphic properties influence soil nutrient availability. Latent variables were created for three categories: experimental factors (ES, SS, ET, and ED), soil properties (WHC, SCC, ISpH, and ISOM), and microplastic characteristics (PC, MPT, MPB, MPS, and MPC).

The model was specified with direct paths from all three latent variables to each nutrient response ratio (ln*RR* for AN, AP, and AK), and indirect paths were evaluated through variable interactions. Model parameters were estimated using maximum likelihood estimation with robust standard errors to account for non-normality in the data distribution. Standardized path coefficients were calculated to enable comparison of effect magnitudes across different measurement scales. Model fit was assessed using multiple indices: chi-square test (χ^2), Comparative Fit Index (CFI), and Root Mean Square Error of Approximation (RMSEA). Acceptable model fit was defined as CFI > 0.90, RMSEA < 0.08, and non-significant χ^2 test ($p > 0.05$). Modification indices were examined to identify potential model improvements, but only theoretically justified paths were added. The analysis was conducted using the "*lavaan*" package (v0.6–12) (Rosseel, 2012).

3. Results

3.1. Overall effects of microplastics exposure on soil available nutrients

The frequency distributions of ln*RR* of AN, AP, and AK followed a Gaussian pattern (Fig. 1a-c), confirming normal distribution under MPs exposure. We found negative effects of MPs exposure on soil nutrient availability across global agricultural systems. MPs significantly reduced AN by 5.3%, AP by 9.4%, and AK by 7.0% relative to uncontaminated

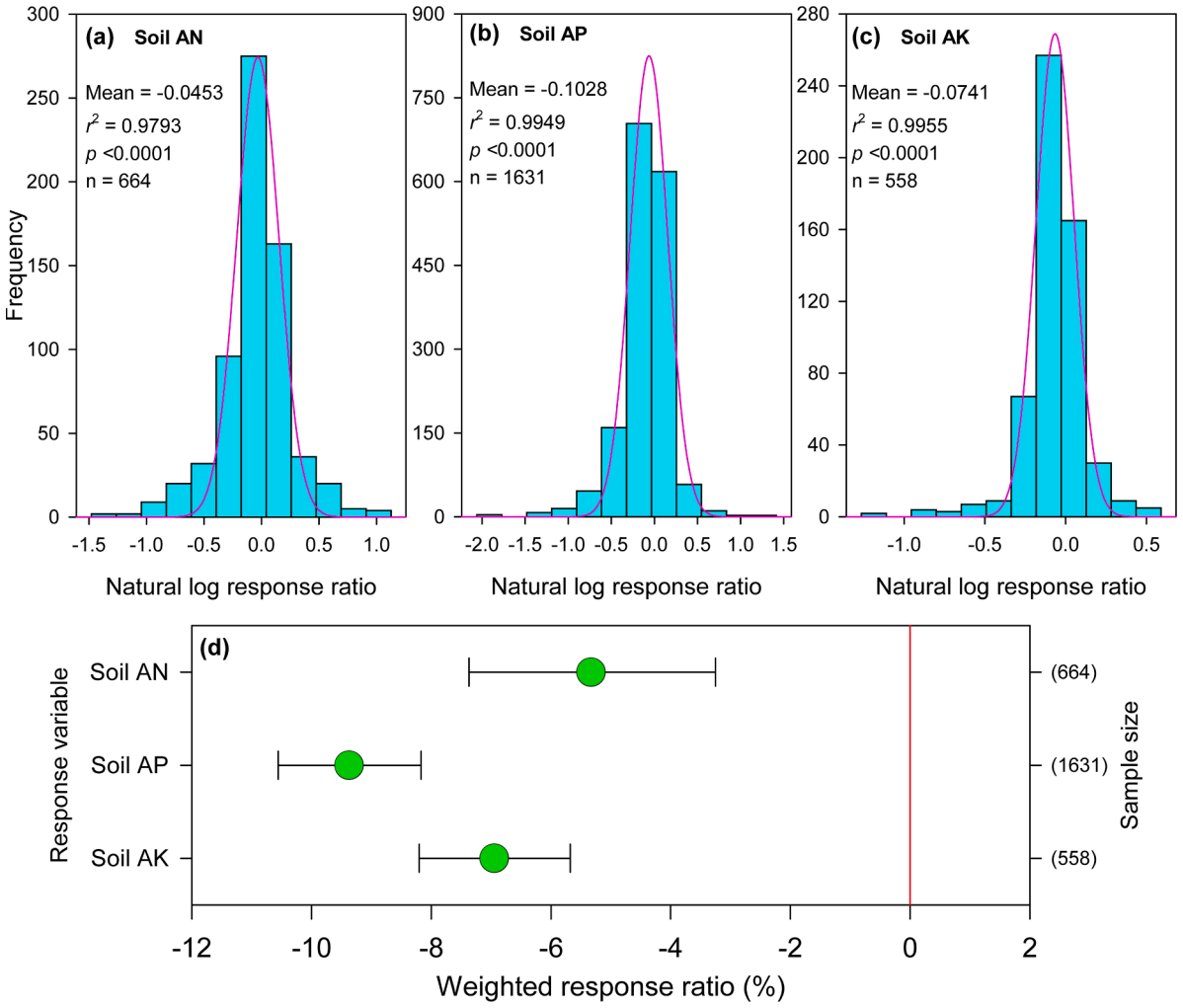

Fig. 1. Frequency distributions of the natural logarithm of response ratios (ln*RR*) for soil available nutrients under microplastics (MPs) exposure: (a) available nitrogen (AN), (b) available phosphorus (AP), and (c) available potassium (AK). The distributions approximate Gaussian patterns, indicating normality in the effect sizes. (d) Overall mean effect sizes (percentage change) of MPs on AN, AP, and AK, with error bars representing 95% confidence intervals (CIs). Negative values indicate depletion relative to controls.

controls (Fig. 1d). Sensitivity analysis excluding studies with MPs concentrations >50 g kg^{-1} (which exceed environmentally relevant levels) confirmed the robustness of overall effects: AP (–8.7%, $p < 0.001$), AK (–6.3%, $p < 0.001$), and AN (–4.9%, $p < 0.01$) remained significantly depleted, indicating that the overall findings are not driven by extreme laboratory concentrations.

3.2. Experimental context affects microplastic-nutrient interactions

Experimental setup significantly influenced effect magnitudes (Fig. 2a-c). Pot experiments reported significant nutrient depletion (AN: –7.5%; AP: –7.6%; AK: –8.4%), while field studies showed no significant changes. Incubation studies suggested selective responses, with significant reductions in AP (–6.4%) and AK (–7.7%) but not AN.

Soil stress status differentially affected nutrient responses (Fig. 2d-f).

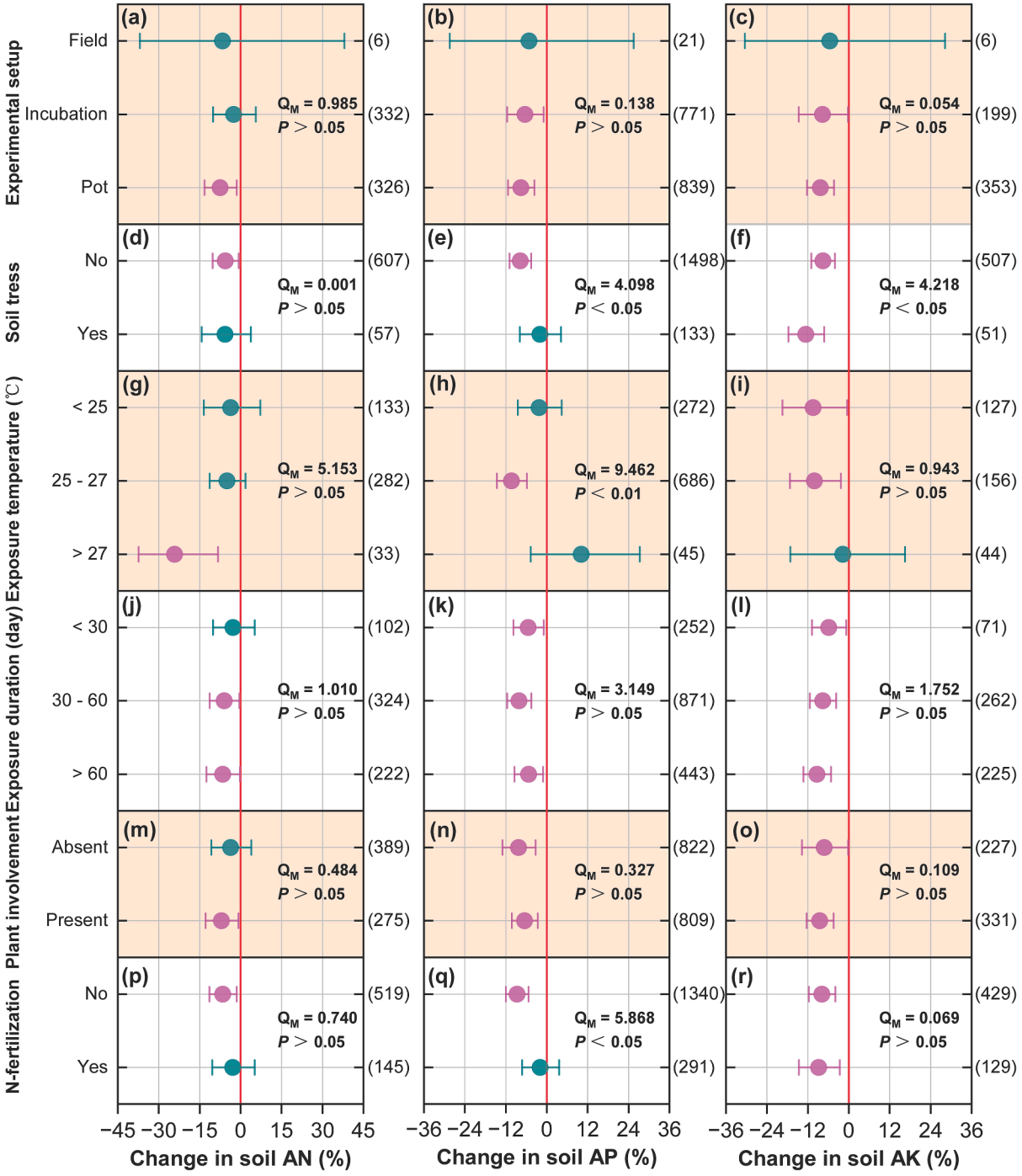

Fig. 2. Moderating effects of experimental factors on microplastics (MPs)-induced changes in soil available nutrients (AN, AP, AK). Panels show percentage changes with 95% confidence intervals for: (a-c) experimental setup (field, pot, incubation); (d-f) soil stress status (pristine *vs.* contaminated); (g-i) exposure temperature (<25 °C, 25–27 °C, >27 °C); (j-l) exposure duration (<30 days, 30–60 days, >60 days); (m-o) plant involvement (present *vs.* absent); (p-r) nitrogen fertilization (yes *vs.* no). Circular markers represent mean effects (weighted response ratio), with error bars indicating 95% confidence intervals (CIs). The vertical red line denotes the zero-effect line. Cyan, pink, and blue circles correspond to neutral, significant negative, and significant positive effects, respectively. Between-group heterogeneity (Q_M) *p*-values are shown where significant ($p < 0.05$). Sample sizes (n) are shown in parentheses on the right.

In pristine soils, MPs significantly reduced AN (–5.6%), AP (–7.8%), and AK (–7.6%) concentrations. In contaminated soils, only AK showed significant depletion (–12.6%).

Temperature emerged as a critical driver, with high temperatures (> 27 °C) inducing AN depletion (–24.3%) compared to moderate (25–27 °C: –5.6%) or low (< 25 °C: –2.8%) temperature conditions (Fig. 2g-i). AP responses were most significant at 25–27 °C (–10.3%), while AK showed consistent depletion across temperature ranges.

Exposure duration (Fig. 2j-l) affected MPs effects, with short-term exposure (< 30 days, Fig. 2j) showing no effect on AN, while intermediate (30–60 days) and prolonged (> 60 days) exposures significantly decreased AN. Both AP and AK (Fig. 2k-l) showed significant reductions across all exposure periods.

Plant presence selectively affected N dynamics, with AN reduction significantly occurring in vegetated systems (–7.0%), while AP and AK decreased regardless of vegetation (Fig. 2m-o). N fertilization mitigated MPs effects (Fig. 2p-r): without additional N, MPs reduced AN (–6.6%) and AP (–8.7%), but these effects were not significant with N addition. AK depletion persisted irrespective of fertilization status.

3.3. Microplastic characteristics drive differential nutrient responses

Polymer composition affected nutrient-specific responses (Fig. 3a-c). PLA and PP caused the most significant AN depletion (–15.0% and –10.2%, respectively). All polymers except PET significantly reduced AP, while AK decreased across most polymer types except PET and PLA.

MPs aging status significantly influenced nutrient responses (Fig. 3d-f), virgin MPs significantly reduced soil AN (–5.2%), AP (–7.3%), and AK (–8.5%). Aged MPs induced significant reductions across all nutrient availability.

Biodegradability assessment showed both conventional and biodegradable MPs significantly decreased AN, AP, and AK (Fig. 3g-i). Conventional MPs reduced AN by –4.6%, AP by –7.9%, and AK by –7.4%. Biodegradable MPs showed comparable or greater effects: AN by –7.4%, AP by –11.2%, and AK by –6.6%.

Size-dependent effects showed critical thresholds (Fig. 3j-l). Small (< 50 μm) and medium (50–150 μm) particles significantly reduced AN and AP, while large particles (> 150 μm) showed no significant effect. AK significantly decreased across all MPs sizes.

MPs concentration showed non-linear concentration effects across nutrients (Fig. 3m-o). Low (–5.5%) and high (–12.2%) MPs concentrations significantly reduced AN (Fig. 3m), whereas medium (–8.3%) and high (–13.5%) concentrations significantly decreased AP (Fig. 3n). AK suggested concentration-independent reduction to MPs exposure (Fig. 3o).

3.4. Edaphic properties control response magnitude and direction

Water holding capacity fundamentally altered MPs impacts (Fig. 4a-c). Under high WHC (> 70%), MPs significantly increased soil AN by 45.2%, whereas under moderate WHC (50–70%), MPs reduced soil AP by 7.2% ($p < 0.05$) and soil AK by 9.8% ($p < 0.05$).

Soil clay content showed complex interactions (Fig. 4d-f): moderate clay (10–20%) showed significant nutrient depletion across all elements, AN (–13.8%), AP (–10.2%), and AK (–9.4%). While high clay (> 20%) increased AN (+36%) while maintaining AP reduction (–8.9%).

Initial soil pH emerged as a critical factor (Fig. 4g-i), with acidic soils (pH < 5.5) showing significant AN depletion (–31.7%) and alkaline soils (pH 7.5–8.5) demonstrating AN enrichment (20.3%, $p < 0.05$), while AP responses shifted from negative in pH 5.5–8.5 soils to positive in highly alkaline conditions (≥8.5; 13.2%, $p < 0.05$), and AK significantly reduced in soil with pH < 8.5.

Soil AN reduction (–34.4%) was significant at 30–40 g kg^{-1} of initial SOM, while AP showed significant reductions across multiple SOM ranges (10–20 g kg^{-1}, –8.1%; 30–40 g kg^{-1}, –11.1%; ≥ 40 g kg^{-1}, –9.2%) and AK showed significant reductions at 10–20 g kg^{-1} (–9.3%), 20–30 g kg^{-1} (–9.2%), and ≥ 40 g kg^{-1} (–9.7%) SOM concentrations (Fig. 4j-l).

3.5. Machine learning indicates dominated controls and non-linear interactions

3.5.1. Model performance and feature importance

XGBoost achieved superior predictive performance among tested algorithms, with test-set R^2 values of 0.62 (AN), 0.59 (AP), and 0.44 (AK) (Fig. 5a-c), and RMSE values of 0.42 (AN), 0.38 (AP), and 0.35 (AK). Feature importance analysis identified hierarchical control structures: initial soil pH dominated AN response (relative importance: 18.4%), while MPs concentration primarily controlled AP (15.2%) and AK (14.8%) dynamics (Fig. 5g-i). Secondary drivers included particle size, exposure duration, and WHC.

3.5.2. SHAP analysis and partial dependence

SHAP value analysis suggested associations between feature values and predicted responses (Fig. 5j-l), indicating patterns consistent with, though not proving, mechanistic hypotheses. Negative SHAP values for pH <6.5 indicated enhanced AN depletion, while positive values at pH > 7.5 suggested mitigation or reversal. Particle size showed consistent negative contributions below 100 μm across all nutrients.

Partial dependence plots with bootstrapped 95% CIs (n = 1000) indicated critical thresholds: MPs size effects plateaued above 100 μm (CIs: 85–115 μm), and concentration impacts saturated beyond 10 g kg^{-1} (CIs: 8.5–12.3 g kg^{-1}) (Fig. 6a-k). Exposure duration showed logarithmic responses, with most changes occurring within 60 days.

3.6. Structural pathways of microplastic impacts

SEM suggested distinct causal pathways governing MPs effects on soil nutrient availability (Fig. 7a). Experimental factors showed the strongest direct effects on nutrient availability, and these effects were positive. Soil properties showed mixed effects: positive influences on AN (path coefficients, $\beta = 0.13$) but negative effects on AK ($\beta = –0.10$), while effects on AP were weak ($\beta = 0.04$). MPs characteristics suggested weak positive effects on AK ($\beta = 0.05$) and marginal effects on other nutrients. Inter-nutrient relationships emerged as significant model components, with pH-dependent regulation evident across all nutrients (Fig. 7b-d). AP responses positively influenced both AN ($\beta = 0.13$) and AK ($\beta = 0.23$) responses. The negative relationship was found between AN and AK responses ($\beta = –0.06$).

4. Discussion

4.1. Microplastics as disruptors of soil major nutrient availability

This global meta-analysis suggests that MPs exposure significantly depletes soil available nutrients, with AP experiencing the most severe reduction (9.4%), followed by AK (7.0%) and AN (5.3%). These suggest substantial agronomic impacts when considered across the 4.9 billion hectares of global agricultural land receiving continuous MPs inputs (Jin et al., 2022; Nizzetto et al., 2016). While the significant contrast between pot/incubation studies and field studies represents a critical interpretive boundary (Fig. 2a-c), this divergence likely reflects three factors: (i) concentration differences between laboratory and field studies; (ii) temporal dynamics, pot experiments (median: 60 days) capture acute responses absent ecosystem buffering and recovery; and (iii) spatial heterogeneity, field soils maintain structural complexity and biological activity that mitigate localized impacts.

The AP depletion aligns with established sorption chemistry principles. Phosphate anions have high affinity for positively charged sites on weathered MPs surfaces, particularly under acidic conditions where surface protonation enhances positive charge density (Wang et al., 2024). This is supported by our finding that acidic soils (pH < 5.5) showed maximum nutrient depletion, while alkaline conditions reversed

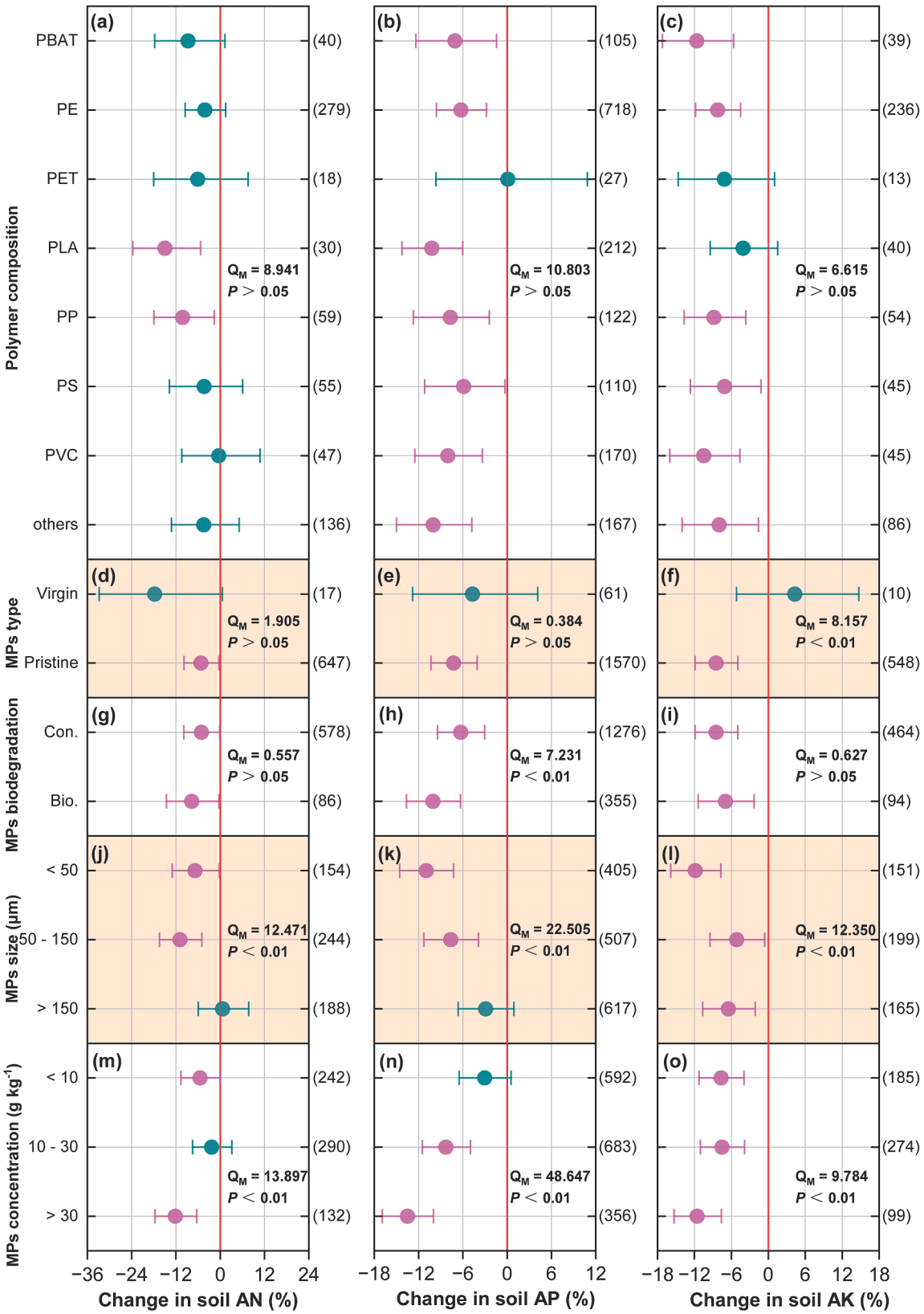

Fig. 3. Influence of microplastics (MPs) characteristics on soil nutrient responses. Panels show effects of: (a-c) polymer composition (PBAT, PE, PET, PLA, PP, PS, PVC, others); (d-f) MPs type (virgin *vs*. aged); (g-i) MPs biodegradation (conventional *vs*. biodegradable); (j-l) MPs size (<50 μm, 50–150 μm, >150 μm); and (m-o) MPs concentration (low: <10 g kg^{-1}, medium: 10–30 g kg^{-1}, high: >30 g kg^{-1}). The vertical red line denotes the zero-effect line. Cyan, pink, and blue circles correspond to neutral, significant negative, and significant positive effects, respectively. Between-group heterogeneity (Q_M) *p*-values are shown where significant ($p < 0.05$). Sample sizes (n) are shown in parentheses on the right.

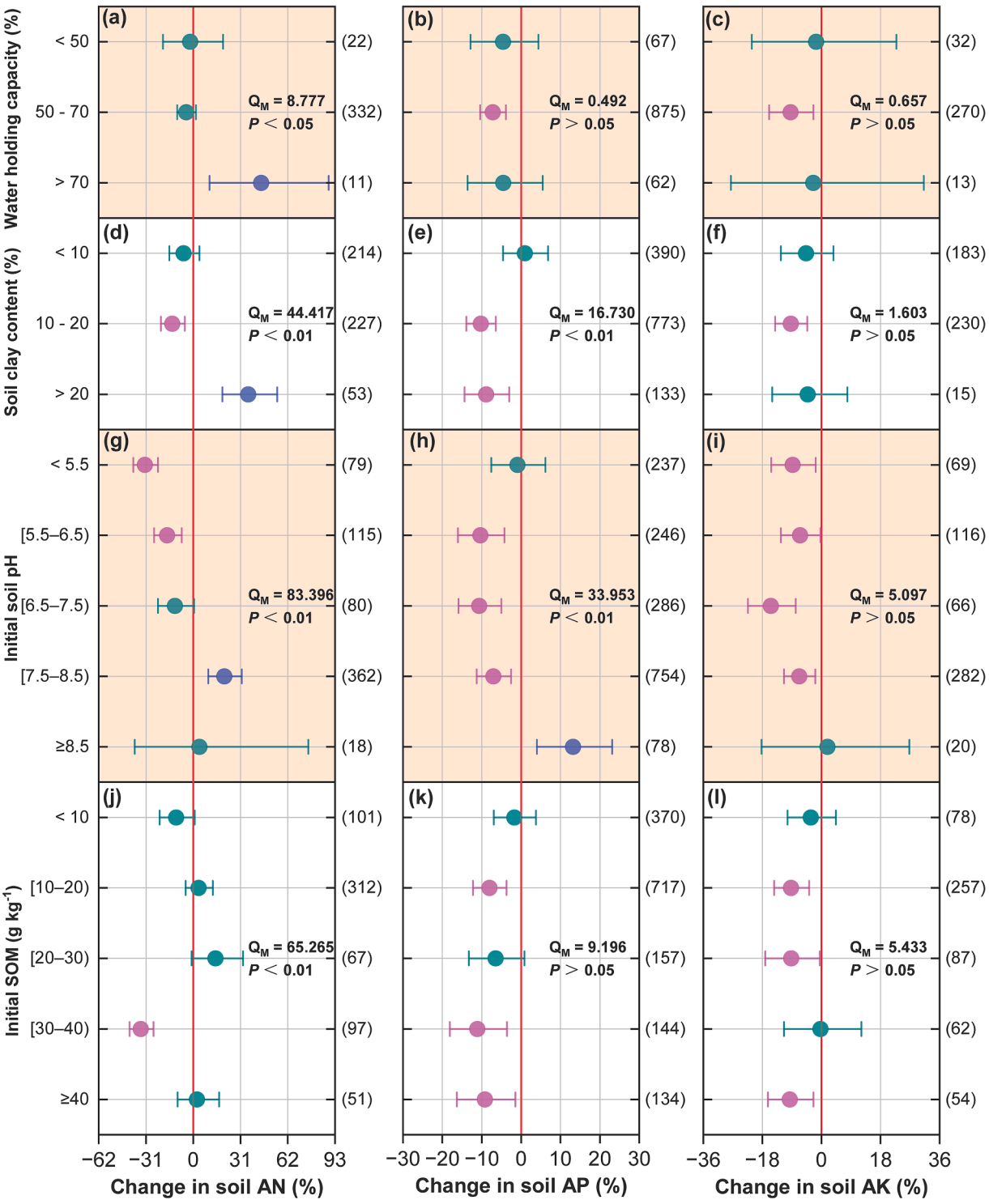

Fig. 4. Edaphic properties affecting microplastic impacts on nutrient availability. Responses vary with: (a-c) water holding capacity (<50%, 50–70%, >70%); (d-f) soil clay content (<10%, 10–20%, >20%); (g-i) initial soil pH (<5.5, 5.5–6.5, 6.5–7.5, 7.5–8.5, ≥8.5); and (j-l) initial soil organic matter (<10, 10–20, 20–30, 30–40, ≥40 g kg^{-1}). The vertical red line denotes the zero-effect line. Cyan, pink, and blue circles correspond to neutral, significant negative, and significant positive effects, respectively. Between-group heterogeneity (Q_M) *p*-values are shown where significant ($p < 0.05$). Sample sizes (n) are shown in parentheses on the right.

or mitigated effects. Recent spectroscopic evidence indicated that weathered polyethylene and polypropylene develop carbonyl and hydroxyl functional groups that serve as phosphate binding sites, with distribution coefficients ranging from 2.3–5.2 L kg^{-1} (Wang et al., 2024; Yin et al., 2023).

The observed nutrient depletion suggests that MPs operate as dynamic surfaces actively sequestering nutrients through synergistic mechanisms (Joo et al., 2021; Rillig et al., 2019; Wang et al., 2024). Beyond direct sorption, MPs create nutrient-depleted microsites through biofilm formation, where microbial communities immobilize nutrients within extracellular polymeric substances (Moyal et al., 2023; Rummel et al., 2017). The size-dependency of effects, particles <50 μm causing maximum depletion, provides quantitative support for this biofilm hypothesis, as smaller particles offer 10–100-fold greater specific surface

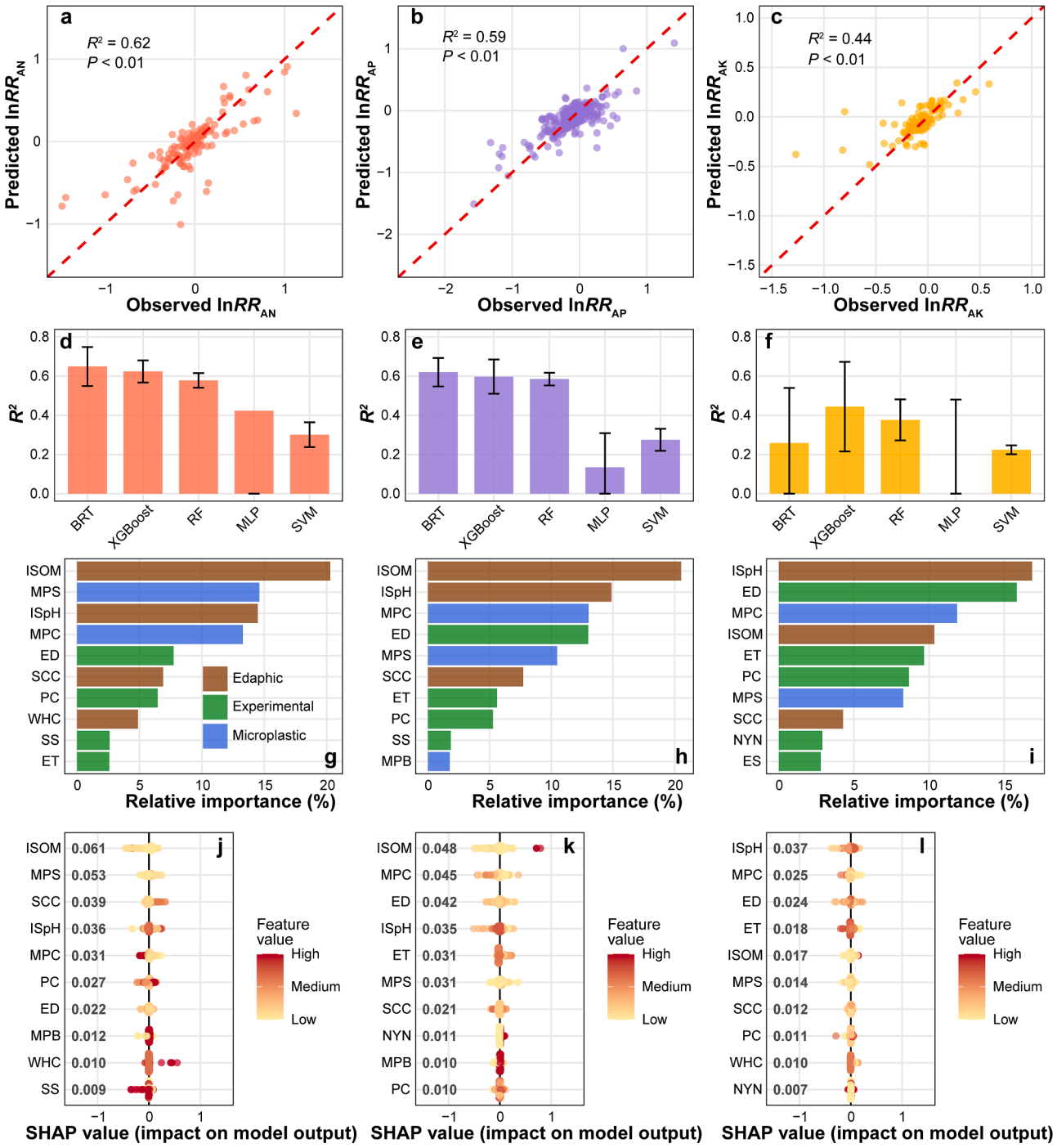

Fig. 5. Machine learning analysis revealing hierarchical controls of microplastic impacts. (a–c) Predicted *vs.* observed ln*RR* for test datasets, with R^2 values of 0.62 (AN), 0.59 (AP), and 0.44 (AK). (d–f) Comparison of predictive performance (R^2) across five algorithms (BRT, XGBoost, RF, MLP, SVM) for each nutrient. (g-i) Feature importance rankings from XGBoost gain metric identifying primary drivers for each nutrient. (j-l) SHAP summary plots showing feature contributions to individual predictions, with color indicating feature values (red: high, blue: low) and x-axis position indicating impact on model output. Abbreviations: ES (experimental setup), SS (soil stress), ET (exposure temperature), ED (exposure duration), Plant (plant involvement), and NYN (N-fertilization), PC (Polymer composition), MPB (MPs biodegradation), MPT (MPs type), MPS (MPs size), MPC (MPs concentration), WHC (Water holding capacity), SCC (soil clay content), ISpH (initial soil pH), ISOM (initial SOM).

area for microbial colonization per unit mass (de Souza Machado et al., 2018; Rummel et al., 2017). Meta-analytic evidence that MPs increase microbial biomass by 8–20% (Fig. 8) indicates that biological immobilization substantially contributes beyond abiotic sorption. The selective AN reduction in vegetated systems (–7.0% *vs.* non-significant without plants) further implicates rhizosphere-specific processes, where root exudates may enhance microbial colonization of MPs surfaces and stimulate N-immobilizing communities.

Three convergent patterns in our meta-analytic data provide indirect evidence for microbial mediation of MPs-nutrient interactions: (i) the size-dependency of effects (maximum depletion by particles <50 μm) is consistent with surface area-controlled biofilm formation; (ii) the time-dependency (AN effects emerging only after >30 days) aligns with typical biofilm maturation timescales of 15–45 days (Moyal et al.,

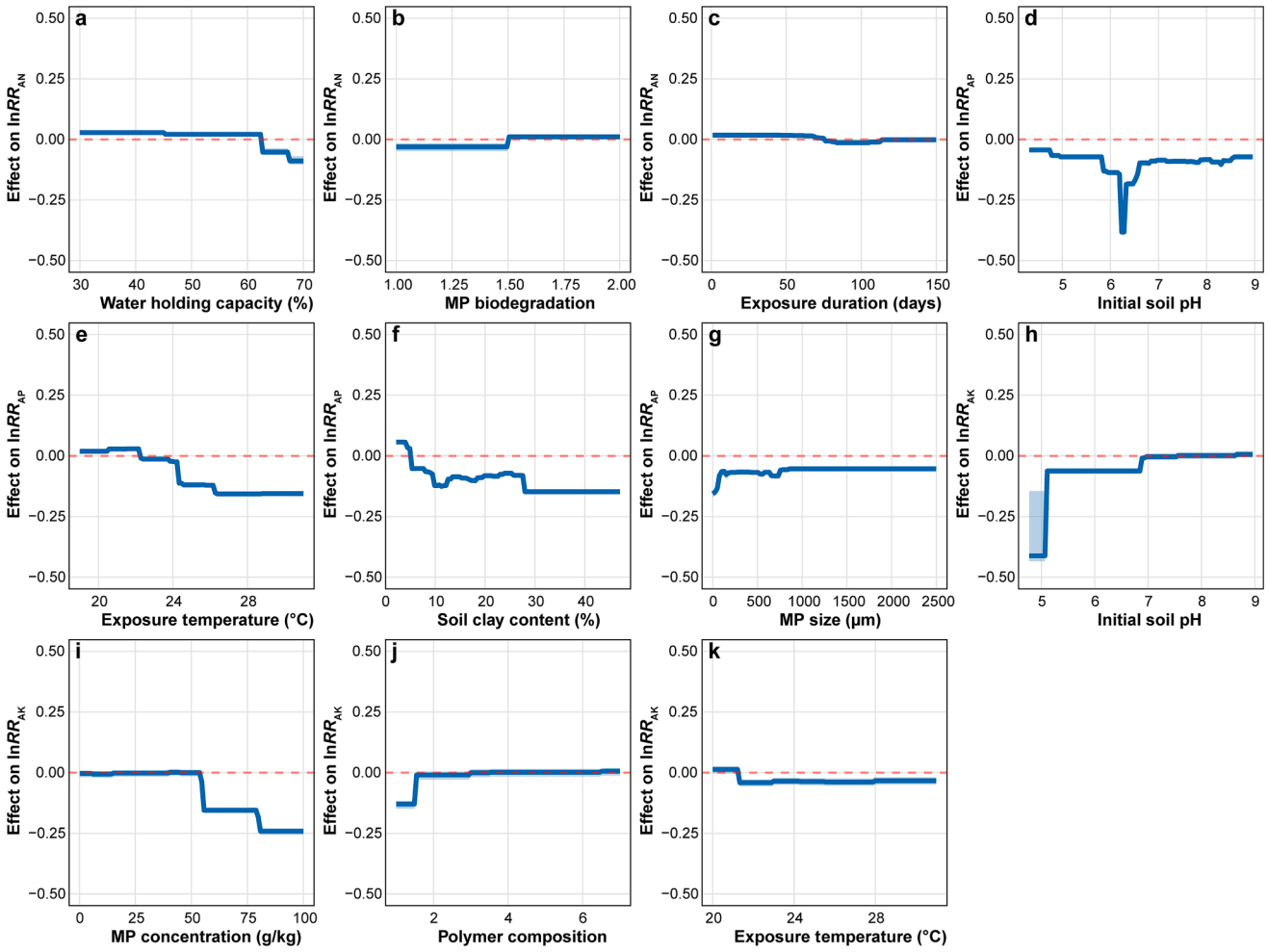

Fig. 6. Partial dependence plots revealing non-linear relationships and interaction effects between key predictors and soil nutrient responses to microplastics. (a-d) One-dimensional partial dependence plots for available nitrogen (AN) showing marginal effects of the top four predictors. (e-h) Corresponding plots for available phosphorus (AP). (i-k) Corresponding plots for available potassium (AK). Blue lines indicate mean effects. Red dashed lines indicate zero effect.

2023); and (iii) the enhanced depletion by biodegradable polymers, which provide metabolizable carbon substrates, supports biological immobilization-microbial communities utilizing polymer carbon would immobilize mineral N and P to maintain stoichiometric balance (C:N ratios of 8–15 in microbial biomass *vs.* >100 in polymer substrates). While these patterns are suggestive rather than definitive, they provide a framework linking our quantitative findings to mechanistic hypotheses that merit direct experimental testing.

4.2. Key moderators, thresholds, and non-linear interactions

The temperature-dependency of MPs effects, particularly the 4.3-fold increase in AN depletion at >27 °C, suggests a concerning positive feedback between climate warming and MPs impacts (Chia et al., 2023; Parvez et al., 2024). This temperature amplification likely reflects thermally-activated processes: accelerated polymer chain scission and additive leaching following Arrhenius kinetics (Bridson et al., 2023; Sun et al., 2019), enhanced microbial metabolic rates with Q_{10} values of 2–3 (Ding et al., 2020; Seeley et al., 2020), and temperature-dependent shifts in nutrient speciation (Afzal et al., 2025). Given IPCC projections of 2–4 °C warming, MPs impacts on nutrient availability will intensify disproportionately in tropical and subtropical agricultural regions.

The machine learning identified thresholds provide quantitative targets for risk-based management: MPs sizes >100 μm show minimal effects, concentrations <10 g kg^{-1} show linear responses amenable to dilution strategies, and exposure durations <30 days allow potential recovery. The identified thresholds represent aggregate patterns across seven polymer types (PE, PS, PVC, PLA, PBAT, PP, PET). However, polymer-specific threshold shifts are expected: biodegradable polymers generating carboxyl-rich surfaces may show lower concentration thresholds for nutrient sorption compared to chemically inert polymers whose reactivity depends on weathering-induced oxidation. Future studies should validate polymer-specific thresholds through targeted factorial experiments.

While initial soil pH acted as the dominant predictor of AN response (18.4%), it performs within a multivariate context: SHAP interaction analysis indicated significant pH × clay content synergies, where high clay soils (>20%) buffered pH-dependent depletion through aggregate-mediated physical protection of nutrient pools from MPs surface sorption (Lehmann et al., 2021). Site-specific assessment should therefore integrate texture, organic matter, and aggregate stability metrics alongside pH.

4.3. Soil–water interface processes and water management implications

Water holding capacity emerged as a significant moderator of MPs effects ($Q_M = 8.777$, $p < 0.05$ for AN), with the reversal from nutrient depletion under moderate WHC (50–70%) to enrichment under high WHC (>70%; AN: +45.2%). This reversal can be attributed to four mechanistic pathways operating under water-saturated conditions: (1) reduced oxygen diffusion limits aerobic polymer chain scission (Beltrán-Sanahuja et al., 2021), suppressing generation of reactive

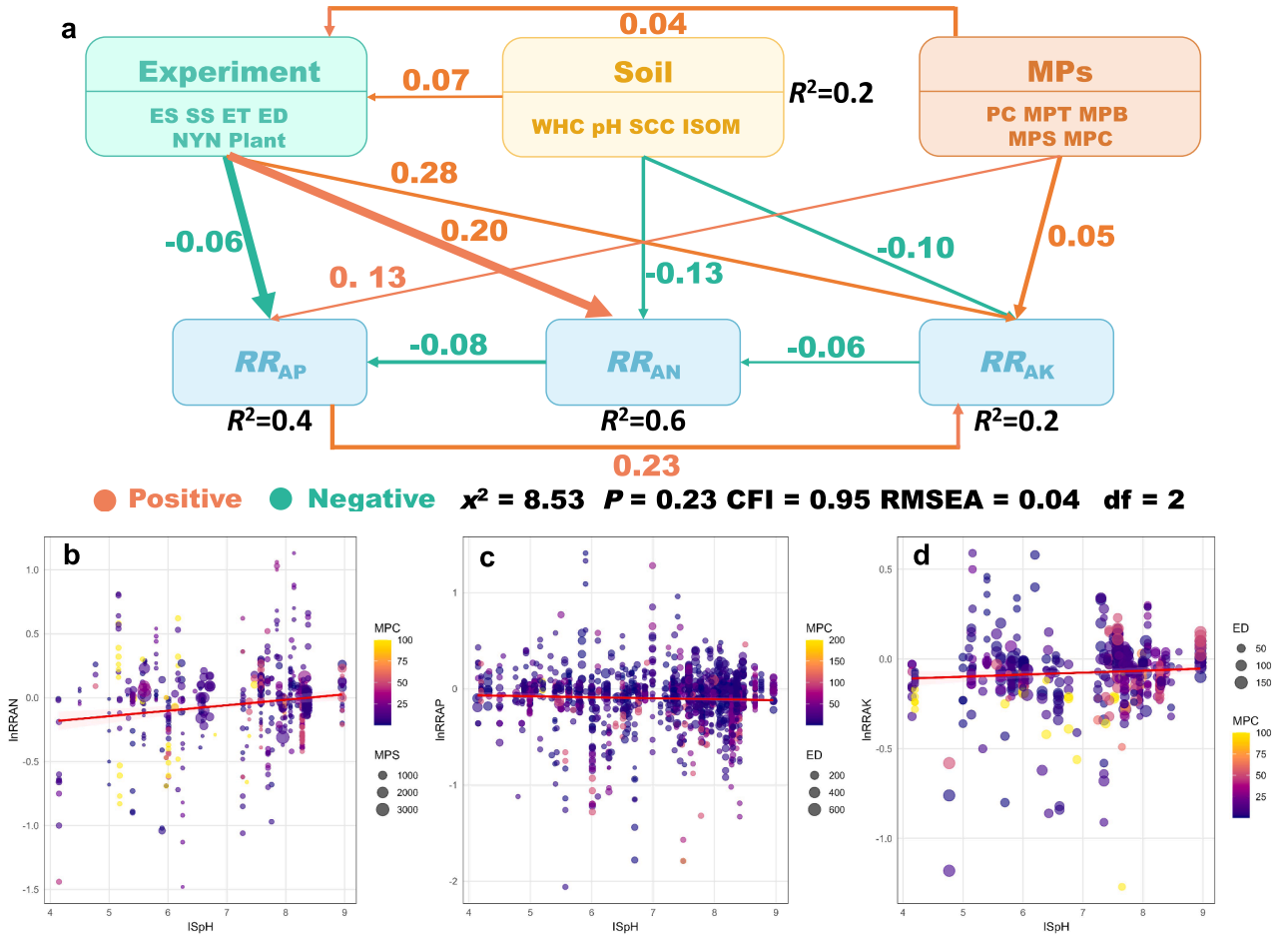

Fig. 7. (a) Structural equation modeling (SEM) revealing direct and indirect pathways of microplastic impacts (MPs) on soil nutrient availability. The model indicates relationships among experimental factors (ES: experimental setup, SS: soil stress, ET: exposure temperature, ED: exposure duration, NYN: nitrogen fertilization), soil properties (WHC: water holding capacity, pH: soil pH, SCC: soil clay content, ISOM: initial soil organic matter), microplastic characteristics (PC: polymer composition, MPT: microplastic type, MPB: microplastic biodegradability, MPS: microplastic size, MPC: microplastic concentration), and response of nutrient availability (RR_{AN}, RR_{AP}, RR_{AK}). Path coefficients indicate standardized effect sizes, with orange arrows representing positive effects and teal arrows representing negative effects. Arrow thickness corresponds to effect magnitude. (b-d) regression showing relationships between initial soil pH and nutrient response ratios, with point size indicating MPS and color gradient representing MPC or ED.

surface functional groups that serve as nutrient binding sites; (2) expanded water films increase effective diffusion distances for nutrient ions to reach polymer surfaces, reducing sorption kinetics (Kaiser et al., 2024; Moyal et al., 2023); (3) anaerobic conditions shift microbial communities toward dissimilatory pathways that release immobilized N and P through reductive dissolution of Fe/Mn-oxyhydroxide–nutrient complexes (Yin et al., 2023); and (4) clay dispersion under saturated conditions releases electrostatically bound nutrients from clay–MPs heteroaggregates (Lehmann et al., 2021).

These findings carry implications for agricultural water management. Irrigation strategies maintaining increased soil moisture may inadvertently mitigate MPs-induced nutrient depletion, while alternating wet–dry cycles, common in paddy systems receiving sewage sludge, could amplify depletion during drying phases when nutrient–MPs surface contact intensifies. For regions relying on treated wastewater irrigation, which simultaneously introduces MPs and nutrients, the net effect on nutrient availability depends on the balance between nutrient loading and MPs-induced sequestration, representing a critical knowledge gap for water reuse management. Soil pH was the dominant predictor identified by machine learning. In acidic soils where impacts are most severe, liming to pH above 6.5 could mitigate MPs-induced depletion by altering polymer surface charge and microbial community structure (Zhao et al., 2021).

4.4. Biodegradable plastics: mechanistic comparison with conventional polymers

The comparable or greater nutrient depletion caused by biodegradable MPs (particularly PLA with 15% AN reduction) challenges current policies promoting these materials as sustainable alternatives, though interpretation requires acknowledging that 89% of biodegradable polymer observations derived from pot studies. This paradox likely stems from accelerated fragmentation rates generating higher surface areas for nutrient sorption, and release of organic acids during hydrolysis that acidify microsites (Fan et al., 2022; Zhao et al., 2025). Recent field studies support these findings, indicating that PBAT and PLA mulches altered N cycling more severely than PE, with 2–10-fold increases in nitrous oxide emissions attributed to carbon priming effects (Greenfield et al., 2022).

Beyond the biodegradability classification, polymer-specific chemistry fundamentally determines nutrient interaction mechanisms. PLA induced the strongest AN depletion (–15.0%), likely through hydrolytic lactic acid generation that acidifies microsites. PVC significantly reduced AP (–10.3%) and AK (–9.8%), consistent with phthalate plasticizer and HCl release. PE and PP showed moderate effects through surface area-dependent sorption, amplified by UV-weathering. PET showed no significant effects, potentially reflecting its high crystallinity

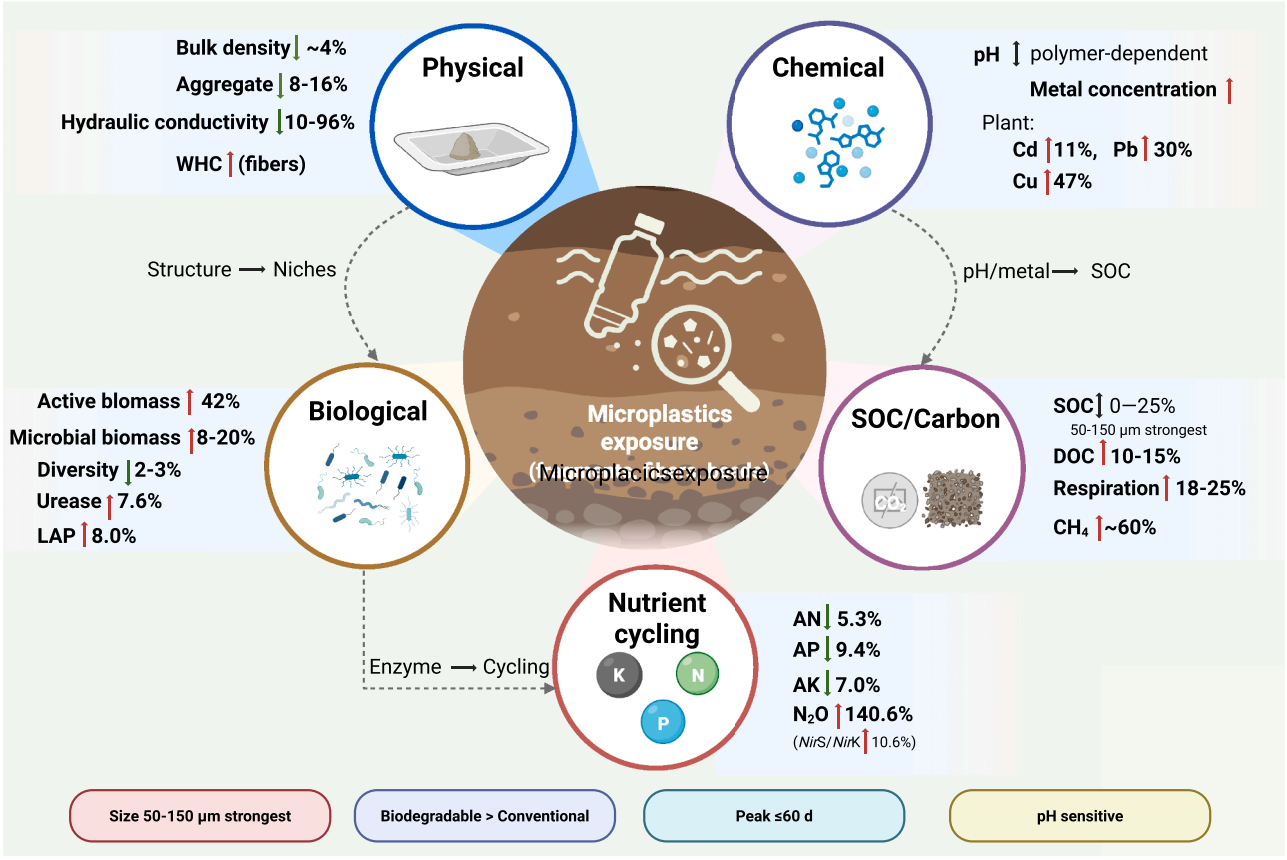

Fig. 8. Microplastics (MPs) reshape soil functioning, values compile our study and recent global meta-analyses (An et al., 2023; Guo et al., 2022; Iqbal et al., 2024b; Liu et al., 2024; Qiu et al., 2022; Su et al., 2023; Xiang et al., 2024, 2025; Zhao et al., 2024). Central node depicts MPs in soil; arrows point to five domains (carbon cycling, nutrient cycling, physical, biological, and chemical properties). Arrow color encodes direction (red = increase; green = decrease; gray = context-dependent), with labels showing pooled effect sizes (transformed % change from ln*RR* where applicable). Abbreviations refer to Fig. 5. LAP, leucine aminopeptidase; N_2O, nitrous oxide; CH_4, methane; DOC, dissolved organic C; Cd, cadmium; Pb, lead; Cu, copper. Most values from controlled studies; field validation pending.

limiting surface weathering. These patterns indicate that chemical composition, rather than biodegradability per se, governs nutrient depletion magnitude and mechanism.

4.5. *Implications for agriculture, policy, and future research*

The integration of machine learning with meta-analysis demonstrates the value of hybrid approaches for understanding complex environmental systems (Fu et al., 2025). Traditional linear models would have missed the pH-dependent sign reversals and synergistic size-concentration interactions that emerged from our analysis. The interpretable framework using SHAP values bridges predictive accuracy and mechanistic understanding (Fazil et al., 2024; Iqbal et al., 2026).

Critical knowledge gaps include: (1) mechanisms underlying nutrient enrichment at high WHC and clay content; (2) long-term data from field experiments spanning multiple cropping cycles; (3) soil active organic matter fractions as moderators of MPs-nutrient interactions; and (4) interactions with warming, N deposition, and drought stress. The current evidence base is temporally constrained (78% of observations ≤60 days), likely overestimating effects relative to field conditions where buffering and adaptation may partially offset depletion.

If laboratory-derived effects were to manifest under field conditions, theoretical yield reductions of 3–8% could occur (Mueller et al., 2012). However, the absence of significant effects in field studies, combined with unrealistic concentrations in many pot experiments, suggests this represents an upper-bound scenario. Our findings support regulatory approaches calibrated to local conditions, prioritizing: (1) acidic soils in warm climates; (2) horticultural systems with intensive plastic use; (3) regions dependent on sewage sludge; and (4) areas with rapid agricultural intensification.

5. Conclusions

This meta-analysis coupled with machine learning found that MPs exposure posed a threat to soil nutrient availability across global agricultural systems, with impacts affected by complex interactions among MPs characteristics, environmental conditions, and edaphic properties. The identification of critical thresholds, non-linear responses, and synergistic interactions provided quantitative guidance for risk assessment and management interventions. As agricultural soils continue accumulating MPs under business-as-usual scenarios, the nutrient depletion effects suggested here threaten to undermine global food security efforts. Action is required to implement source control, develop sustainable alternatives, and establish monitoring programs before irreversible degradation of soil fertility occurs. The machine learning framework developed here offered an insight for assessing complex environmental interactions that could be applied to other emerging contaminants, advancing predictive understanding of anthropogenic impacts on Earth's critical zone.

CRediT authorship contribution statement

Yangzhou Xiang: Writing – original draft, Visualization, Validation, Methodology, Funding acquisition, Formal analysis, Data curation, Conceptualization. **Josep Peñuelas:** Writing – review & editing, Conceptualization. **Matthias C. Rillig:** Writing – review & editing,

Funding acquisition, Conceptualization. **Xuqiang Luo:** Writing – review & editing, Software, Investigation, Funding acquisition, Conceptualization. **Luca Nizzetto:** Writing – review & editing, Funding acquisition. **Jarkko Akkanen:** Writing – review & editing. **Ying Liu:** Writing – review & editing, Conceptualization. **Yang Luo:** Writing – review & editing, Conceptualization. **Bin Yao:** Writing – review & editing, Resources, Project administration, Funding acquisition, Conceptualization. **Yuan Li:** Writing – review & editing, Writing – original draft, Visualization, Investigation, Formal analysis, Conceptualization.

Declaration of competing interest

The authors declare that they have no known competing financial interests or personal relationships that could have appeared to influence the work reported in this paper.

Acknowledgements

This work was supported by Natural Science Foundation of China (32260725), Fundamental Research Funds for the Guizhou Provincial Science and Technology Projects (QKHJC-ZK [2022] YB335), and Guizhou Education University Scientific Research Fund Project (2024YB002; 2024BSKQ003). Matthias C. Rillig acknowledges funding from the project μPlastic (031B0907A) from the Bundesministerium für Bildung und Forschung. Josep Peñuelas was supported by the Spanish Government grant PID2022-140808NB-I00, funded by MCIN, AEI/10.13039/501100011033 European Union Next Generation EU/PRTR. Luca Nizzetto was supported by the PAPILLONS project (No 101000210).

Supplementary materials

Supplementary material associated with this article can be found, in the online version, at doi:10.1016/j.watres.2026.126056.

Data availability

Data will be made available on request.

References

Afzal, M., Tan, X., Fang, M.L., Jin, W., Liang, Q., Wang, X., Chen, X., Zhang, X., Tan, Z., 2025. High temperatures and microplastic enhanced inorganic phosphorus mineralization and phoD-harboring bacterial abundance in paddy soil. Ecotoxicol. Environ. Saf. 302, 118495.

An, Q., Zhou, T., Wen, C., Yan, C., 2023. The effects of microplastics on heavy metals bioavailability in soils: a meta-analysis. J. Hazard. Mater. 460, 132369.

Beltrán-Sanahuja, A., Benito-Kaesbach, A., Sánchez-García, N., Sanz-Lázaro, C., 2021. Degradation of conventional and biobased plastics in soil under contrasting environmental conditions. Sci. Total Environ. 787, 147678.

Bergmeir, C., Benítez, J.M., 2012. Neural networks in R using the stuttgart neural network simulator: RSNNS. J. Stat. Softw. 46 (7), 1–26.

Boots, B., Russell, C.W., Green, D.S., 2019. Effects of microplastics in soil ecosystems: above and below ground. Environ. Sci. Technol. 53 (19), 11496–11506.

Bridson, J.H., Abbel, R., Smith, D.A., Northcott, G.L., Gaw, S., 2023. Impact of accelerated weathering on the leaching kinetics of stabiliser additives from microplastics. J. Hazard. Mater. 459, 132303.

Chen, L., Yu, L., Li, Y., Han, B., Zhang, J., Tao, S., Liu, W., 2022. Spatial distributions, compositional profiles, potential sources, and intfluencing factors of microplastics in soils from different agricultural farmlands in china: a national perspective. Environ. Sci. Technol. 56 (23), 16974.

Chen, T., Guestrin, C., 2016. XGBoost: a scalable tree boosting system. In: Krishnapuram, B., et al. (Eds.), Proceedings of the 22nd ACM SIGKDD International Conference on Knowledge Discovery and Data Mining, pp. 785–794.

Chia, R.W., Lee, J.-Y., Lee, M., Lee, G.-S., Jeong, C.-D., 2023. Role of soil microplastic pollution in climate change. Sci. Total Environ. 887, 164112.

de Souza Machado, A.A., Kloas, W., Zarfl, C., Hempel, S., Rillig, M.C., 2018. Microplastics as an emerging threat to terrestrial ecosystems. Glob. Chang. Biol. 24 (4), 1405–1416.

de Souza Machado, A.A., Lau, C.W., Kloas, W., Bergmann, J., Bachelier, J.B., Faltin, E., Becker, R., Görlich, A.S., Rillig, M.C., 2019. Microplastics can change soil properties and affect plant performance. Environ. Sci. Technol. 53 (10), 6044–6052.

Ding, L., Mao, R., Ma, S., Guo, X., Zhu, L., 2020. High temperature depended on the ageing mechanism of microplastics under different environmental conditions and its effect on the distribution of organic pollutants. Water. Res. 174, 115634.

Duval, S., Tweedie, R., 2000. Trim and fill: a simple funnel-plot–Based method of testing and adjusting for publication bias in meta-analysis. Biometrics 56 (2), 455–463.

Fan, P., Yu, H., Xi, B., Tan, W., 2022. A review on the occurrence and influence of biodegradable microplastics in soil ecosystems: are biodegradable plastics substitute or threat? Environ. Int. 163, 107244.

Fazil, A.Z., Gomes, P.I.A., Sandamal, R.M.K., 2024. Applicability of machine learning techniques to analyze microplastic transportation in open channels with different hydro-environmental factors. Environ. Pollut. 357, 124389.

Freitas, B., D'Amelio, P.B., Milá, B., Thébaud, C., Janicke, T., 2025. Meta-analysis of the acoustic adaptation hypothesis reveals no support for the effect of vegetation structure on acoustic signalling across terrestrial vertebrates. Biol. Rev. 100 (2), 815–833.

Fu, X., Sun, J., Tian, K., Liu, Y., Zhang, H., 2025. Predicting the sorption capacity of perfluoroalkyl and polyfluoroalkyl substances in soils: meta-analysis and machine learning modeling. Environ. Sci. Technol. 59 (33), 17699–17710.

Fuller, S., Gautam, A., 2016. A procedure for measuring microplastics using pressurized fluid extraction. Environ. Sci. Technol. 50 (11), 5774–5780.

Greenfield, L.M., Graf, M., Rengaraj, S., Bargiela, R., Williams, G., Golyshin, P.N., Chadwick, D.R., Jones, D.L., 2022. Field response of N_2O emissions, microbial communities, soil biochemical processes and winter barley growth to the addition of conventional and biodegradable microplastics. Agric. Ecosyst. Environ. 336, 108023.

Greenwell, B.M., 2017. pdp: an R package for constructing partial dependence plots. R J. 9, 421–436.

Guo, Z., Li, P., Yang, X., Wang, Z., Lu, B., Chen, W., Wu, Y., Li, G., Zhao, Z., Liu, G., Ritsema, C., Geissen, V., Xue, S., 2022. Soil texture is an important factor determining how microplastics affect soil hydraulic characteristics. Environ. Int. 165, 107293.

Hedges, L.V., Gurevitch, J., Curtis, P.S., 1999. The meta-analysis of response ratios in experimental ecology. Ecology. 80 (4), 1150–1156.

Hinsinger, P., Brauman, A., Devau, N., Gérard, F., Jourdan, C., Laclau, J.-P., Le Cadre, E., Jaillard, B., Plassard, C., 2011. Acquisition of phosphorus and other poorly mobile nutrients by roots. Where do plant nutrition models fail? Plant Soil. 348 (1), 29–61.

Iqbal, S., Worthy, F.R., Gui, H., Li, Y., 2026. Simulating carbon and nitrogen cycling in microplastic contaminated agroecosystems using gradient boost regression model. Circ. Agric. Syst. 6 (1), e005.

Iqbal, S., Xu, J., Gui, H., Bu, D., Alharbi, S.A., Khan, S., Nadir, S., 2024a. Interactive effects of microplastics and typical pollutants on the soil-plant system: a mini-review. Circ. Agric. Syst. 4 (1), e007.

Iqbal, S., Xu, J., Saleem Arif, M., Shakoor, A., Worthy, F.R., Gui, H., Khan, S., Bu, D., Nader, S., Ranjitkar, S., 2024b. Could soil microplastic pollution exacerbate climate change? A meta-analysis of greenhouse gas emissions and global warming potential. Environ. Res. 252, 118945.

Jin, T., Tang, J., Lyu, H., Wang, L., Gillmore, A.B., Schaeffer, S.M., 2022. Activities of microplastics (MPs) in agricultural soil: a review of MPs pollution from the perspective of agricultural ecosystems. J. Agric. Food Chem. 70 (14), 4182–4201.

Joo, S.H., Liang, Y., Kim, M., Byun, J., Choi, H., 2021. Microplastics with adsorbed contaminants: mechanisms and treatment. Environ. Chall. 3, 100042.

Kaiser, S., Kaegi, R., Rhein, F., 2024. Influence of aging, morphology and particle size on the behavior of microplastics during magnetic seeded filtration. Sci. Total Environ. 957, 177353.

Knapp, S., van der Heijden, M.G.A., 2018. A global meta-analysis of yield stability in organic and conservation agriculture. Nat. Commun. 9 (1), 3632.

Lajeunesse, M.J., 2016. Facilitating systematic reviews, data extraction and meta-analysis with the metagear package for R. Methods Ecol. Evol. 7 (3), 323–330.

Lan, G., Huang, X., Li, T., Huang, Y., Liao, Y., Zheng, Q., Zhao, Q., Yu, Y., Lin, J., 2025. Effect of microplastics on carbon, nitrogen and phosphorus cycle in farmland soil: a meta-analysis. Environ. Pollut. 370, 125871.

Lehmann, A., Leifheit, E.F., Gerdawischke, M., Rillig, M.C., 2021. Microplastics have shape- and polymer-dependent effects on soil aggregation and organic matter loss – an experimental and meta-analytical approach. Microplast. nanoplast. 1 (1), 7.

Liao, X., Kang, H., Haidar, G., Wang, W., Malghani, S., 2022. The impact of biochar on the activities of soil nutrients acquisition enzymes is potentially controlled by the pyrolysis temperature: a meta-analysis. Geoderma 411, 115692.

Liaw, A., Wiener, M., 2002. Classification and regression by randomForest. R news 2 (3), 18–22.

Liu, X., Yu, Y., Yu, H., Sarkar, B., Zhang, Y., Yang, Y., Qin, S., 2024. Nonbiodegradable microplastic types determine the diversity and structure of soil microbial communities: a meta-analysis. Environ. Res. 260, 119663.

Liu, Y., Just, A., 2019. SHAPforxgboost: SHAP plots for 'XGBoost'. R package version 0.1.3.

Lundberg, S.M., Lee, S.-I., 2017. A unified approach to interpreting model predictions. In: Guyon, I., et al. (Eds.), Proceedings of the 31st International Conference on Neural Information Processing Systems, 30, pp. 4765–4774.

Moyal, J., Dave, P.H., Wu, M., Karimpour, S., Brar, S.K., Zhong, H., Kwong, R.W.M., 2023. Impacts of biofilm formation on the physicochemical properties and toxicity of microplastics: a concise review. Rev. Environ. Contam. Toxicol. 261 (1), 8.

Mueller, N.D., Gerber, J.S., Johnston, M., Ray, D.K., Ramankutty, N., Foley, J.A., 2012. Closing yield gaps through nutrient and water management. Nature 490 (7419), 254–257.

Nizzetto, L., Futter, M., Langaas, S., 2016. Are agricultural soils dumps for microplastics of urban origin? Environ. Sci. Technol. 50 (20), 10777–10779.

Parvez, M.S., Ullah, H., Faruk, O., Simon, E., Czédli, H., 2024. Role of microplastics in global warming and climate change: a review. Water Air Soil Pollut. 235 (3), 201.
Qiu, Y., Zhou, S., Zhang, C., Zhou, Y., Qin, W., 2022. Soil microplastic characteristics and the effects on soil properties and biota: a systematic review and meta-analysis. Environ. Pollut. 313, 120183.
R Core Team, 2024. R: a language and environment for statistical computing. R Foundation for Statistical Computing, Vienna.
Rillig, M.C., Lehmann, A., de Souza Machado, A.A., Yang, G., 2019. Microplastic effects on plants. New Phytol. 223 (3), 1066–1070.
Rosseel, Y., 2012. lavaan: an R package for structural equation modeling. J. Stat. Softw. 48 (2), 1–36.
Rummel, C.D., Jahnke, A., Gorokhova, E., Kühnel, D., Schmitt-Jansen, M., 2017. Impacts of biofilm formation on the fate and potential effects of microplastic in the aquatic environment. Env., Sci, Technol.Env. Sci Technol Lett 4 (7), 258–267.
Seeley, M.E., Song, B., Passie, R., Hale, R.C., 2020. Microplastics affect sedimentary microbial communities and nitrogen cycling. Nat. Commun. 11 (1), 2372.
Sterne, J.A.C., Egger, M., 2001. Funnel plots for detecting bias in meta-analysis: guidelines on choice of axis. J. Clin. Epidemiol. 54 (10), 1046–1055.
Su, P., Bu, N., Liu, X., Sun, Q., Wang, J., Zhang, X., Xiang, T., Chu, K., Zhang, Z., Cao, X., Li, Z., 2024. Stimulated soil CO2 and CH4 emissions by microplastics: a hierarchical perspective. Soil Biol. Biochem. 194, 109425.
Su, P., Gao, C., Zhang, X., Zhang, D., Liu, X., Xiang, T., Luo, Y., Chu, K., Zhang, G., Bu, N., Li, Z., 2023. Microplastics stimulated nitrous oxide emissions primarily through denitrification: a meta-analysis. J. Hazard. Mater. 445, 130500.
Sun, B., Hu, Y., Cheng, H., Tao, S., 2019. Releases of brominated flame retardants (BFRs) from microplastics in aqueous medium: kinetics and molecular-size dependence of diffusion. Water. Res. 151, 215–225.
Suthaharan, S., 2016. Machine learning models and algorithms for big data classification. Thinking with Examples for Effective Learning. Springer, New York, NY, USA, pp. 1–359.
Viechtbauer, W., 2010. Conducting meta-analyses in R with the metafor package. J. Stat. Softw. 36 (3), 1–48.
Wang, B., Wu, L., Pang, K., Zhang, G., Xu, D., Sun, H., Yin, X., 2024. Transport of reduced PBAT microplastics in saturated porous media: synergistic effects of enhanced surface energy and roughness. Water. Res. 267, 122514.
Wang, P.-Y., Zhao, Z.-Y., Xiong, X.-B., Wang, N., Zhou, R., Zhang, Z.-M., Ding, F., Hao, M., Wang, S., Ma, Y., Uzamurera, A.G., Xiao, K.-W., Khan, A., Tao, X.-P., Wang, W.-Y., Tao, H.-Y., Xiong, Y.-C., 2023. Microplastics affect soil bacterial community assembly more by their shapes rather than the concentrations. Water. Res. 245, 120581.
Wang, T., Zhao, S., Zhu, L., McWilliams, J.C., Galgani, L., Amin, R.M., Nakajima, R., Jiang, W., Chen, M., 2022. Accumulation, transformation and transport of microplastics in estuarine fronts. Nat. Rev. Earth Environ. 3 (11), 795–805.
Wei, H., Xiang, Y., Liu, Y., Zhang, J., 2017. Effects of sod cultivation on soil nutrients in orchards across china: a meta-analysis. Soil Tillage Res. 169, 16–24.
Xiang, Y., Peñuelas, J., Sardans, J., Liu, Y., Yao, B., Li, Y., 2023. Effects of microplastics exposure on soil inorganic nitrogen: a comprehensive synthesis. J. Hazard. Mater. 460, 132514.
Xiang, Y., Rillig, M.C., Peñuelas, J., Sardans, J., Liu, Y., Yao, B., Li, Y., 2024. Global responses of soil carbon dynamics to microplastic exposure: a data synthesis of laboratory studies. Environ. Sci. Technol. 58 (13), 5821–5831.
Xiang, Y., Yao, B., Peñuelas, J., Sardans, J., Nizzetto, L., Li, R., Liu, Y., Luo, Y., Räty, M., Long, J., Li, Y., 2025. Microplastic effects on soil nitrogen cycling enzymes: a global meta-analysis of environmental and edaphic factors. J. Hazard. Mater. 484, 136677.
Yin, M., Yan, B., Wang, H., Wu, Y., Wang, X., Wang, J., Zhu, Z., Yan, X., Liu, Y., Liu, M., Fu, C., 2023. Effects of microplastics on nitrogen and phosphorus cycles and microbial communities in sediments. Environ. Pollut. 318, 120852.
Yu, H., Zhang, Y., Tan, W., Zhang, Z., 2022. Microplastics as an emerging environmental pollutant in agricultural soils: effects on ecosystems and human health. Front. Environ. Sci. 10, 855292.
Zhang, D., Liu, X., Huang, W., Li, J., Wang, C., Zhang, D., Zhang, C., 2020. Microplastic pollution in deep-sea sediments and organisms of the western pacific ocean. Environ. Pollut. 259, 113948.
Zhao, S., Rillig, M.C., Bing, H., Cui, Q., Qiu, T., Cui, Y., Penuelas, J., Liu, B., Bian, S., Monikh, F.A., Chen, J., Fang, L., 2024. Microplastic pollution promotes soil respiration: a global-scale meta-analysis. Glob. Chang. Biol. 30 (7), e17415.
Zhao, T., Lozano, Y.M., Rillig, M.C., 2021. Microplastics increase soil pH and decrease microbial activities as a function of microplastic shape, polymer type, and exposure time. Front. Environ. Sci. 9, 675803.
Zhao, X., Wu, X., Wang, Q., Wu, F., 2025. Ecological risks of biodegradable plastics. Science (1979) 388 (6751), 1034.